NANOMATERIALS
SCIENCE & ENGINEERING
Vol. 7, No. 1, pp. 20-25 (2025)

RESEARCH ARTICLE

https://doi.org/10.34624/nmse.v7i1.37201

The influence of T-Shape flow deflector placement on convection heat transfer over an array heated blocks

AMIRAT Hamza[1,*], KORICHI Abdelkader [1] and AMIRAT Moustapha [2]

[1]*University of Yahia Fares, Laboratory of Mechanics, Physics and Mathematical Modeling (LMP2M) Medea, Algeria*
[2] *Ecole Militaire Polytechnique, Algiers, Algeria*

**Corresponding author, e-mail address: amirat.hamza@gmail.com*

Received 30 July November 2024; accepted 15 January 2025; published online 31 January 2025

ABSTRACT

In this research, a numerical study was conducted to examine the convective heat transfer in a horizontal channel containing multiple heated blocks. The channel design incorporates T-shaped flow deflectors strategically positioned downstream of each block. Air, with a Prandtl number of 0.71 and consistent thermal properties, is used for cooling. The geometric attributes and arrangement of the flow deflectors remain consistent throughout the analysis. The computations are based on a Reynolds number of 400, with systematic variations in the positions of the flow deflectors. The finite volume method, implemented using Ansys Fluent© software, is employed to solve the governing mathematical equations numerically. The results emphasize the significant impact of adjustments to the flow deflector configuration on both fluid flow patterns and heat transfer characteristics across the heated blocks.

1. INTRODUCTION

The temperature rise is a significant concern in various engineering disciplines, such as nuclear power, electronics, and mechanical engineering. Higher temperatures can negatively impact the efficiency and lifespan of engineering products. As a result, thermal engineers are compelled to develop and improve innovative strategies to enhance cooling processes. The existing literature is rich in studies addressing this challenge. For example, Bergles et al. [1] outline 13 methodologies to improve heat transfer in industrial settings. Similarly, Yeh [2] provides a concise overview of the cooling techniques commonly used in the electronics industry. A substantial body of research, as cited in [3-8], has focused on heat transfer dynamics across multiple heated blocks. In a specific study, Herman and Kang [9] investigated the effectiveness of curved deflectors in manipulating airflow to displace warm air trapped between blocks, thereby enhancing heat transfer efficiency. While their results showed positive effects on heat transfer, they also noted a corresponding increase in pressure losses, estimating it to be two to three times higher than scenarios without curved deflectors. Additionally, their findings indicated a correlation between improved heat transfer and higher Reynolds numbers. This concept of curved deflectors as a method for enhanced heat transfer, despite the associated increase in pressure loss, was further supported by numerical and experimental investigations conducted by Lorenzini-Gutierrez et al. [10] and Luviano-Ortiz et al. [11]. Based on the insights derived from the preceding literature review, a considerable body of research has focused on enhancing heat transfer over heated blocks through the use of diverse flow deflectors and vortex promoters. In light of this, the current study seeks to explore the influence of varying positions of T-shaped flow deflectors on convective heat transfer across an array of heated blocks.

2. PHYSICAL MODEL AND MATHEMATICAL FORMULATION

2.1. Setups and Description

In this study, Figure 1a depicts the physical model under investigation. The system's geometric layout features two parallel plates (2D) housing five heated blocks. All measurements are unitless, relative to the channel width H. The heated blocks share identical dimensions (w=h=H/4=0.25). Furthermore, distinct flow deflectors are mounted behind each block; their shapes and sizes are detailed in Figure 1b. Each deflector is positioned at h/2 intervals along the longitudinal axis after every block and at a h distance along the transverse axis. The channel's walls are designed as adiabatic surfaces, except for the heated blocks' base, which experiences a uniform heat flux. At the inlet of the channel (u_{inlet}), a forced flow is implemented. The channel is divided into two parts before and after the blocks, with lengths denoted as L_{in}=3 and L_{out}=20, respectively. Due to the significant disparity in the third dimension compared to the others, we simplify the problem by treating it as a two-dimensional (2D) scenario.

Assuming a constant, laminar, and incompressible flow, the fluid's thermophysical properties are constant and it follows Newtonian laws. The corresponding mathematical formulas for the physical model in a non-dimensional format can be organized as follows, assuming that buoyancy and viscous dissipation are ignored:

Mass:

$$\frac{\partial u}{\partial x}+\frac{\partial v}{\partial y}=0 \tag{1}$$

x-momentum:

$$\mathrm{Re}\left(u\frac{\partial u}{\partial x}+v\frac{\partial u}{\partial y}\right)=-\frac{\partial p}{\partial x}+\left(\frac{\partial^2 u}{\partial x^2}+\frac{\partial^2 u}{\partial y^2}\right) \tag{2}$$

y-momentum:

$$\mathrm{Re}\left(u\frac{\partial v}{\partial x}+v\frac{\partial v}{\partial y}\right)=-\frac{\partial p}{\partial y}+\left(\frac{\partial^2 v}{\partial x^2}+\frac{\partial^2 v}{\partial y^2}\right) \tag{3}$$

Energy:
The fluid phase:

$$P_e\left(u\frac{\partial \theta_f}{\partial x}+v\frac{\partial \theta_f}{\partial y}\right)=\left(\frac{\partial^2 \theta_f}{\partial x^2}+\frac{\partial^2 \theta_f}{\partial y^2}\right) \tag{4}$$

The solid phase:

$$\frac{k_{sl}}{k_f}\left(\frac{\partial^2 \theta_{sl}}{\partial x^2}+\frac{\partial^2 \theta_{sl}}{\partial y^2}\right)=0 \tag{5}$$

Non-dimensional variables:

$$x=\frac{x^*}{H^*};\ y=\frac{y^*}{H^*};\ u=\frac{u^*}{u_m^*};\ v=\frac{v^*}{u_m^*};$$
$$\theta=\frac{(T-T_0)}{(q''.H^*/k_f)};\ p=\frac{p^*.H}{\mu_f\,.\,u_m^*} \tag{6}$$

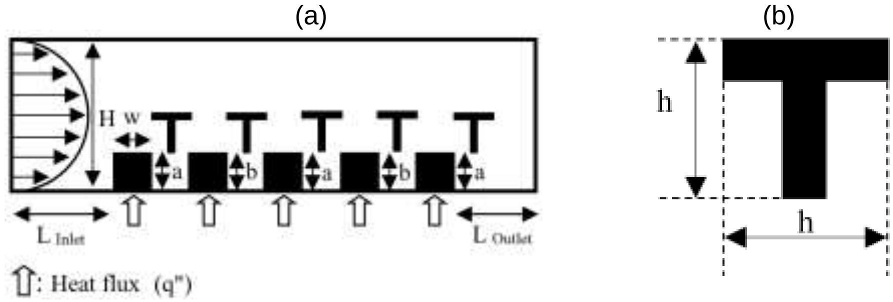

Figure 1. (a): Physical domain channel; (b): Geometric of the **T-shape** deflector.

Table 1. Boundary conditions.

	Border of the geometry	Boundary conditions
Hydrodynamic conditions	Inlet	$\frac{\partial p}{\partial x}=0;\ U_{inlet}=6y(1-y);$ $v=0$
	Outlet	$\frac{\partial u}{\partial x}=\frac{\partial v}{\partial x}=0;$ The pressure is equal to the ambient pressure
	Channel walls Block bases Solid-Fluid interface	$u=v=0$
Thermal conditions	Inlet	$\theta_f=0$
	Outlet Channel walls	$\frac{\partial \theta_f}{\partial x}=0$
	Block bases	q"= 1
	Solid-Fluid interface	$\theta_f=\theta_{sl};$ $k_f\frac{\partial \theta_f}{\partial n}=k_{sl}\frac{\partial \theta_{sl}}{\partial n}$

And the relevant non-dimensional numbers are:

$$Re=\frac{\rho_f.u_m.H}{\mu_f};\ Pr=\frac{\mu_f.c_{p_f}}{K_f};\ Pe=Re.Pr \qquad (7)$$

2.2. Boundary Conditions

Table 1 provides a condensed compilation detailing the boundary conditions.
Selecting L_{in}=3 and L_{out}=20 arises from an extensive analysis, where calculations delved into diverse scenarios incorporating different inlet and outlet distances.

2.3. Numerical Solution and Validation

The solution of the governing equations within the described physical model is reached numerically utilizing the finite volume approach. Ansys Fluent® serves as the platform for simulation, employing the Simple algorithm. The validation assessments of grid independence and accuracy of computations have been conducted in previous studies [12], using local Nusselt numbers. The results of grid configuration 1,350 × 110 are judged to satisfy Re=400 requirements. Furthermore, close alignment with the research conducted by Young and Vafai is demonstrated, with a maximum deviation of less than 3%. Iterative calculations are conducted until convergence states are achieved. The residuals for every independent parameter are constrained to 10^{-6}.

3. RESULTS AND DISCUSSION

Computational simulations are conducted for flow deflectors with T-shapes at a Reynolds number 400. The outcomes regarding streamlines, temperature profiles, and the mean Nusselt number (derived from equation 9) are presented.

$$Nu_x=\frac{h_c.H^*}{k_f}=-\frac{1}{\theta_s}.\frac{\partial \theta_f}{\partial n} \qquad (8)$$

$$\overline{Nu}=\frac{1}{A}\int_A Nu_s\,ds \qquad (9)$$

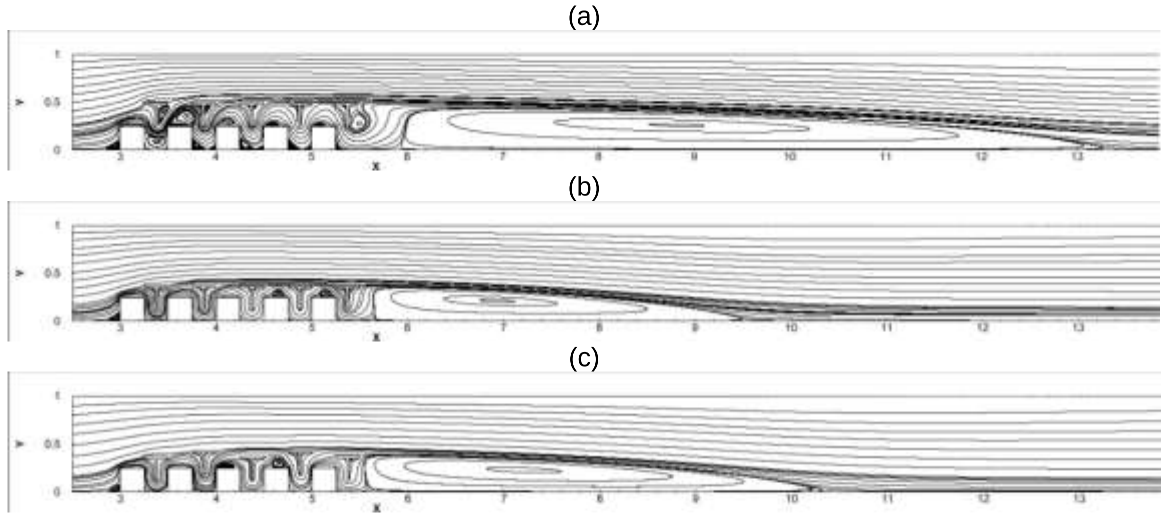

Figure 2. Streamlines for T-shaped deflectors at Re=400, with different deflector positions: (a) a=b=0.25, (b) a=b=0.125, (c) a=0.125; b=0.253.

3.1. Streamlines

In Figure 2, when the distance between the flow deflectors and the bottom of the cavity is decreased to a=b=0.25, also for the flow deflectors position a=0.125 and b=0.25, the flow penetrates more deeply into the gaps between the blocks. Figures 2b and 2c illustrate the case of a=b=0.125, where all vortices between the blocks are completely eliminated. It is evident that the largest vortex, located after the last deflector, decreases in size as the distances a and b decrease to 0.125. This reduction in size causes the vortex to move closer to the last deflector, almost halfway. It is important to note that in the case of a=b=0.25, some of the vortices above the blocks' faces are eliminated, while others are displaced to the right of the blocks' central axes. This change in vortex behavior occurs when the flow deflector positions change to a=b=0.125 (Figures 2b) and a=0.125; b=0.25 (Figures 2c). In the scenario where a=0.25 and b=0.125 (refer to Figure 3.1C), the vortex behind the last block's deflector moves to the left, positioning itself right next to the deflector. Furthermore, it increases in size compared to the case where a=b=0.125 but remains smaller than when a=b=0.25.

It's crucial to understand that reducing the distance between the deflectors and the base of the cavities limits the flow passage section between the blocks and the deflectors. This causes the airflow speed to increase in these areas, improving heat transfer through convection. The same effect occurs when the distance between the last blocks and the vortex after the last deflector is reduced. Thus, it is very important to note that all vortices near the blocks present areas of heat accumulation. The deflectors minimize the mixing of fluid airflow by separating the airflow around the blocks from the airflow above the deflectors. This phenomenon could negatively affect heat transfer through the blocks.

3.2. Isotherms contours

As shown in Figure 3, the temperature of the solid and fluid phases increases as the vertical distance between the deflectors and the bottom of the cavities decreases to a=b=0.125. This leads to isolating the airflow around the blocks from the airflow above the deflectors. This effect is more noticeable in the fourth and fifth blocks due to the increased of heat loaded by the cooling fluid in these regions. Let's consider the case where the positions of the deflectors are a=0.125 and b=0.25, as shown in Figure 3c. These deflector positions allow the airflow to move more freely and improve the mixing and contact of the hot airflow around the blocks with the cooler airflow above the deflectors. This improves the heat transfer between the two airflows, thereby increasing the heat transfer around the blocks compared to the case with the

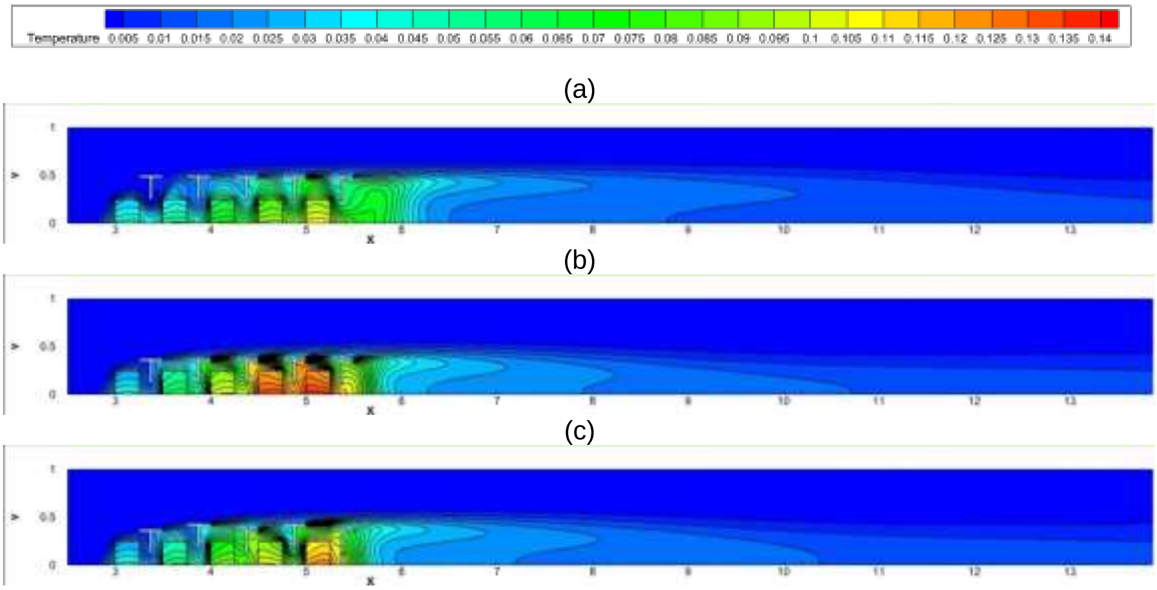

Figure 3. Isotherm contours for T-shaped deflectors at Re=400, with different deflector positions: (a) a=b=0.25, (b) a=b=0.125, (c) a=0.125; b=0.25.

deflectors positioned at a=b=0.125. The best position for optimal cooling is the case where a=b=0.25, followed by the position a=0.125 and b=0.25. The worst cooling condition corresponds to the position a=b=0.125. It is important to note that the positions of the deflectors influence the shape of the temperature contours inside and outside the heated blocks.

3.3. Mean Nusselt Number

Heat transfer is countified using the mean Nusselt number, presented in Figure 4. The position of T-

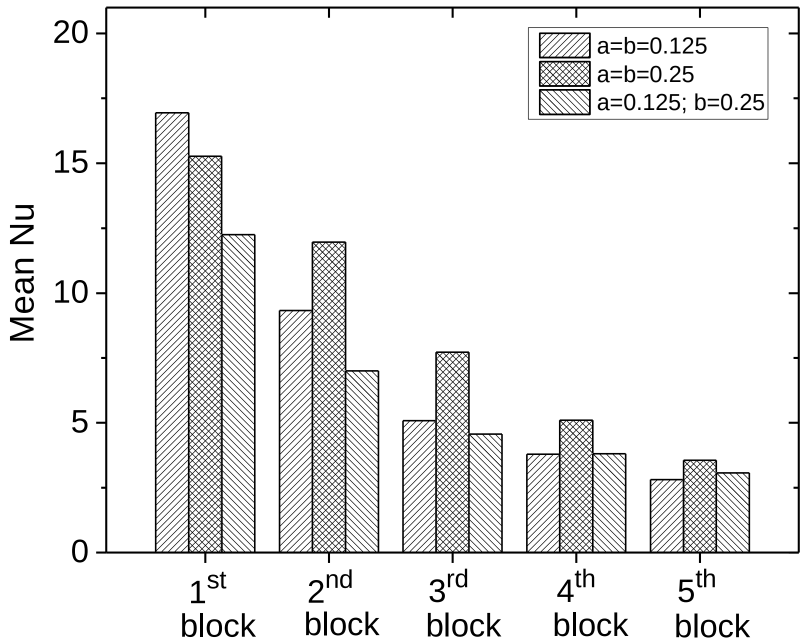

Figure 4 The average Nusselt numbers for the cases with and without T-shaped deflectors.

shaped deflectors has a considerable effect on heat transfer. For the first block, position a=b=0.125 gives the best heat transfer, followed by position a=b=0.025, and then the case with position a=0.125 and b=0.25. Regarding the other blocks, the highest heat transfer is observed with the deflectors at position a=b=0.25, followed by the deflectors at position a=b=0.125, except for the fourth block, which shows that the heat transfer for the deflectors at positions a=b=0.125 and a=0.125, b=0.25 is approximately the same. The same applies to the last block but with finer variations. The change in heat transfer behavior with different deflector positions between the first block and the others occurs because the cooling air around the blocks experiences a temperature increase due to low mixing and separation provided by the deflectors.

4. CONCLUSION

The study used numerical simulations to analyze fluid flow and forced heat transfer over heated blocks with T-shaped flow deflectors. It aimed to investigate the influence of the deflectors' position at a Reynolds number of Re=400. The simulations examined three positions of the flow deflectors and highlighted the significant impact of the deflectors' position on flow and thermal fields.

The deflectors effectively eliminate vortices in the space between the blocks, especially when properly shaped and positioned. Vortices typically form on the upper faces of the heated blocks. Moreover, the vortex following the last deflector is directed away from the rear face of the last block. Eliminating vortices near the blocks could potentially enhance heat transfer around the blocks through improved convection in these regions. The presence of deflectors diminishes the flow mixing, consequently impairing heat transfer efficiency in the terminal three blocks. Such reduction in flow mixing attenuates the enhancement in heat transfer that could be achieved through the augmented thermal energy transported by the fluid. The most unfavorable position for cooling the blocks is a=b=0.125. The results are clearer for the fourth and fifth blocks. The most effective cooling configuration is attained when the values of both variables a and b are precisely set to 0.25. For the initial block, optimal thermal efficiency, indicated by the highest mean Nusselt number, occurs at a=b=0.125. Conversely, suboptimal thermal performance is observed at a=b=0.25. Subsequent evaluations reveal that a configuration of a=b=0.25 emerges as the preferable setup, optimizing thermal efficiency across the remaining blocks.

REFERENCES

[1] A.E. Bergles, V. Nirrnalan, G.H. Junkhan, and R.L. Webb, Bibliography on augmentation of convective heat and mass transfer II, Heat Transfer Laboratory Report HTL-31, ISU-ERI-Ames- 84221, Iowa State University, Ames (1983).
[2] L. Yeh, J. Electron. *Packag*.**117**, 333–339 (1995).
[3] J. Young, and K. Vafai, *J. Heat Transfer*, **12**, 34–42 (1999).
[4] T. J. Young, and K. Vafai, *Int. J. Heat Mass Transf.*, **41**, 3279–3298 (1998).
[5] J. S. Nigen, and C. H. Amon, *J. Fluids Eng.*, **116**, 499–507 (1994).
[6] G. Imani, M. Maerefat, and K. Hooman, *Numeri. Heat Transf. A Appl.*, **62**, 798–821 (2012).
[7] J. Davalath, and Y. Bayazitoglu, *J. Heat Transfer*, **109**, 321–328 (1987).
[8] F. P. Incropera, *J. Heat Transfer*, **110**, 1097–1111 (1988).
[9] C. Herman, and E. Kang, *Int. J. Heat Mass Transf.*, ***45***, *3741–3757 (2002).*
[10] D. Lorenzini-Gutierrez, A. Hernandez-Guerrero, J. L. Luviano-Ortiz, and J. C. Leon-Conejo, *Appl. Therm. Eng.*, **75**, 800–808 (2015).
[11] L. Luviano-Ortiz, A. Hernandez-Guerrero, C. RubioArana, and R. Romero-Mendez, *Int. J. Heat Mass Transf.*, **51**, 972–3984 (2008).
[12] H. Amirat, and A. Korichi, *Journal of Mechanics*, **36**, 19-131 (2020).